

A Combined Experimental and Computational Investigation of Hydrogen-Bonded 2,7-Diazaindole-(Water)_{1,2} Complexes Isolated in the Gas Phase

Simran Baweja,^a Bhavika Kalal^a and Surajit Maity*,^a

Abstract: We have presented a detailed experimental and computational analysis on the 1:1 and 1:2 complexes of 2,7-diazaindole (27DAI) with water in the gas phase. The complexes were characterized using two-color-resonant two-photon ionization (R2PI), laser induced fluorescence (LIF), single vibronic level fluorescence (SVLF), and photoionization efficiency spectroscopic methods. The 0_0^0 band of the $S_1 \leftarrow S_0$ electronic transition of 27DAI-H₂O complex was observed at 33074 cm⁻¹, largely red shifted by 836 cm⁻¹ compared to that of the bare 27DAI. From the R2PI spectrum, the detected modes at 141 (ν'_{Tx}), 169 (ν'_{Ty}) and 194 (ν'_{Ry}) cm⁻¹ were identified as the internal motions of H₂O molecule in the complex. However, these modes were detected at 115 (ν''_{Tx}), 152 (ν''_{Ty}) and 190 (ν''_{Ry}) cm⁻¹ in the ground state which suggested a stronger hydrogen bonding interaction in the photo-excited state. The structural determination was aided by the detection of ν_{NH} and ν_{OH} values in the ground and excited state complex using the FDIR and IDIR spectroscopies. The detection of ν_{NH} at 3414 and ν_{OH} at 3447 cm⁻¹ in 27DAI-H₂O have shown an excellent correlation with the most stable structure consisting of N(1)-H...O and OH...N(7) hydrogen bonded bridging water molecule in the ground state. The structure of the complex in the electronic excited state (S_1) were confirmed by corresponding bands at 3210 (ν_{NH}) and 3265 cm⁻¹ (ν_{OH}). The IR-UV hole burning spectroscopy confirmed the presence of only one isomer in the molecular beam. The ionization energy (IE) of the 27DAI-H₂O complex was obtained as 8.789±0.001 eV, which was significantly higher than the 7AI-H₂O complex. The 1:2 complex 27DAI-(H₂O)₂ was identified by a strong transition at 32565 cm⁻¹, which was red shifted by 1345 cm⁻¹. The corresponding FDIR spectrum resulted three bands at 3207, 3261 and 3385 cm⁻¹, which are assigned as the hydrogen bonded ν_{NH} of 27DAI and two ν_{OH} vibrations from solvent-bridge connecting N(1)H and N(7) groups. The obtained structures of 27DAI-H₂O and 27DAI-(H₂O)₂ have explicitly shown the formation of cyclic one- and two-solvent bridges incorporating N(1)-H...O and O-H...N(7) hydrogen bonds upon micro solvation. The lower excitation and higher ionization energies of the 27DAI-H₂O complex compared to 7AI-H₂O established higher stabilization of N-rich molecules. The solvent clusters forming linear bridge between the hydrogen/proton acceptor and donor sites in the complex can be considered a stepping stone to investigate the photoinduced tautomerization of N-bearing biologically relevant molecules.

1 Introduction

Understanding the photochemistry of nucleobases has been the topics of interest as they undergo mutations via a cascade of mechanisms upon UV absorption.¹⁻⁵ For example, the photoinduced tautomerization reaction pathways, via excited state hydrogen and/or proton transfer, have been recognized as a potential mutation processes. Despite several destructive processes, naturally selected biomolecules have high photo stability due to the existence of efficient non-radiative relaxation mechanisms.^{6,7} For example, the nucleobases, such as adenine, guanine, cytosine, thymine and uracil, undergo excited state deactivation via internal conversion, which is driven by the puckering of heterocycles.⁸⁻¹¹ To gain insights into such underlying self-defence mechanisms, it is essential to isolate the photoactive part of the molecule and systematically investigate various intrinsic molecular properties.

Investigations have been carried out in both solution and gas phase on how the photo-physics of the nucleobase can be affected by the solvent environment. A large number of theoretical studies

are available that examine the effect of water molecules on the purine nucleobases.¹²⁻¹⁴ But due to the relative complexity of forming the nucleobase-solvent clusters in the gas phase, a very few experimental studies have been reported in the literature focussing on the role of intrinsic solvent molecules.^{15,16} However, to surpass this limitation, analogues molecules that possess the ability to mimic such nucleobases, have been used for long time to understand such hydrogen bonded solvent-chromophore interactions.

7-azaindole (7AI) has been one such prototypic system which was explored extensively due to its resemblance to the nucleobases such as adenine and guanine. Its dimer, (7AI)₂, is known to mimic the reactions involved in the photo mutagenesis of DNA base pairs.¹⁷⁻²³ Sekiya et al. reported a series of molecular clusters of 7-azaindole in the gas phase such as 7AI-(H₂O)₂, 7AI-(CH₃OH)₂ and 7AI-(C₂H₅OH)₂ which shed light upon the role of solvents in the excited state processes.²⁴⁻²⁶ In the recent years, a derivative of 7AI i.e. 2,7-diazaindole (27DAI) has been studied due to the substitution of nitrogen on the 2nd position.²⁷ In the previous article on isolated 2,7-diazaindole, we emphasized on its increased photostability due to the increase in the N-content and the higher photo acidity of the

N(1)-H_a group, in comparison to its parent molecule 7AI.²⁸ Further, several theoretical and solution phase studies have been done which concluded the lowering of excited state hydrogen/proton transfer energy barriers in the solvent clusters of 27DAI compared to that of 7AI.²⁹ The experimental investigations are limited to very few solvation phase studies of 2,7-diazaindole.

In this article, we extend our investigation to the micro-solvated water clusters of 2,7-diazaindole i.e., 27DAI-(H₂O)_{1,2} isolated in the gas phase. We aim to probe the hydrogen-bonded ground and excited state structures of isolated 2,7-diazaindole-water (27DAI-H₂O)_{1,2} complexes, which will be a suitable candidate for hydrogen and proton transfer reactions in the excited state. To achieve that, we have recorded a two-color resonant two-photon ionization spectrum (R2PI) and laser-induced fluorescence (LIF) spectra, revealing the vibrational energy levels in the excited state of 27DAI-(H₂O)_{1,2} complex. We have employed single vibronic level fluorescence (SVLF) spectroscopy to comprehend the ground state structure of the 27DAI-H₂O complex. We have also performed photoionization efficiency spectroscopy to determine the ionization energy (I.E.) of the 27DAI-H₂O complex. Further, 2,7-diazaindole molecule has two major competing binding sites due to the presence of N-group at 2nd as well as 7th position on the indole ring which makes them favourable to undergo various excited state reactions. Based on this, we have explored the various docking site preferences of the hydrogen bonded clusters of 27DAI-(H₂O)_{1,2} using IR-UV double resonance spectroscopy. The most favourable structures of the 27DAI-(H₂O)_{1,2} clusters were obtained using computational calculations to supplement the experimental findings. Additionally, we have done a thorough comparison of the 27DAI molecular complexes with the reported hydrogen bonded water complexes of 7-azaindole by Kaya et al.³⁰ The structural analysis presented in this study would aid in the elucidation of the energetics involved in formation of various excited state hydrogen/proton transfer products leading to the deactivation of such N-H rich chromophores.

2 Methods

2.1 Experimental

The 27DAI-H₂O complex was formed via the co-expansion of 27DAI vapours and water seeded in 2 bars of He, in a pulsed supersonic jet. The 27DAI was heated to 358 K to achieve sufficient vapour pressure for the experiment. The solvent holder was placed at 273-278 K to maximize the formation of size-selective 1:1 and 1:2 clusters, using a Peltier setup. The detailed experimental setup was described earlier.³¹ The jet cooled molecular complexes were excited using a frequency-doubled tunable dye laser output, which was pumped by the second harmonic of an Nd:YAG laser. A second Nd:YAG laser was used to pump (a) a subsequent UV laser used for the ionization and (b) a tunable IR-OPO. The photoionization efficiency spectrum was recorded to determine the ionization potential of the 1:1 complex. The S₁ ← S₀ excitation spectrum of the 27DAI-H₂O complex was then measured using 2C-R2PI spectroscopy by monitoring the m/z ratio of 137 amu and scanning the excitation laser wavelength. Further, laser-induced fluorescence (LIF) spectrum was recorded for the 27DAI-(H₂O)₂ complex. The SVLF spectrum was recorded by keeping the excitation laser wavelength fixed at the band origin and the fluorescence emission was dispersed using a 1.5 m spectrometer to understand the ground state structure of the complex. The ground (S₀) and excited (S₁) state N-H and O-H vibrational frequencies were detected using resonant ion-dip infrared (IDIR) and fluorescence-dip

infrared (FDIR) techniques. To isolate the isomeric 1:1 molecular complex, IR-UV hole-burning spectrum was recorded where IR laser wavelength was fixed at the ground state ν_{NH} frequency of the complex 20 ns prior to the scanning excitation laser. Any dip originating from the depleted ground state were identified by the reduced intensities on comparing the same spectra obtained without the hole-burning IR laser. All the experiments were performed with ~0.2 mJ/pulse of UV and 5 mJ/pulse of IR laser power with a beam size of ~2 mm. The bandwidths of the dye laser outputs were ~0.3 cm⁻¹ in the visible region. The resolution of the spectrometer was 0.02 nm at the slit width of 100 μm used for the experiment. The UV-VIS OPO used for ionization and IR-OPO has a resolution of ~0.1 nm and 5 cm⁻¹ respectively. The 500 mm focusing lens was used in front of ionization laser during the experiment. The R2PI experiments were conducted using fifth harmonic of Nd:YAG output (1064 nm) at 213 nm as the ionization laser, which was generated by mixing of 532 nm and 355 nm using a BBO crystal.

2.2 Computational

All the ground and excited state calculations were performed with the TURBOMOLE program using resolution-of-the-identity (RI) approximation.³² The geometries were optimized using the dispersion corrected density functional theory (DFT-D4) method with the B3LYP density functional and def2-TZVPP basis set. The obtained structures were confirmed without any imaginary harmonic vibrational frequencies. All time-dependent density functional theory (TDDFT) were performed using the random phase approximation. The SCF energy convergence and the optimization thresholds for changes in the energy were set to 10⁻⁶ E_h with the changes in the gradient at 10⁻⁴ E_h/a₀. The optimized S₀ and S₁ geometries were utilized to perform the Franck-Condon simulations for the R2PI and SVLF spectra of 27DAI-H₂O complex. The simulations were performed using the FC-LabWin program developed by Puglisi et al.³³ The resolution of the simulated spectrum was set at 0.5 cm⁻¹ to compare with the experimental spectral bandwidth. The scaling values for N-H and O-H frequencies are obtained from the ratio of experimental and computationally obtained frequencies of 27DAI monomer for both ground and excited states.

3 Results and Discussion

3.1 Two-color resonant two-photon ionization (R2PI) spectroscopy

The R2PI spectrum of 27DAI-H₂O complex, as shown in Figure 1, was recorded in the spectral region of 32950–34670 cm⁻¹ by integrating the (27DAI-H₂O)⁺ ion signal at the mass-to-charge ratio of 137 amu. The band origin for the S₁ ← S₀ electronic transition (0₀⁰) is positioned at 33074 cm⁻¹. The 0₀⁰ transition of the 27DAI monomer (Figure 1a) recorded under the same experimental conditions appeared at 33910 cm⁻¹.²⁸ Therefore, the 0₀⁰ band of the 1:1 complex is red shifted by 836 cm⁻¹, suggesting the higher stabilization of 27DAI-H₂O complex in the excited state relative to the ground state. A similar observation of the large redshift of the band origin of water and methanol complexes of 2,2'-pyridylbenzimidazole was also reported.^{34,35} The red-shift also implies that the H₂O is hydrogen bonded to the N(1)-H_a and N(7) sites of the chromophore. This is similar to that of 7-azaindole-H₂O (7AI-H₂O) complex, where the band origin at 33354 cm⁻¹ was red shifted by 1274 cm⁻¹ compared to the bare 7AI (0₀⁰ at 34628 cm⁻¹).³⁰ The lower redshift of the 0₀⁰ band in 27DAI-H₂O complex is most likely due to the lower hydrogen bond energy in 27DAI-H₂O in the excited state than that in the 7AI-H₂O (SI

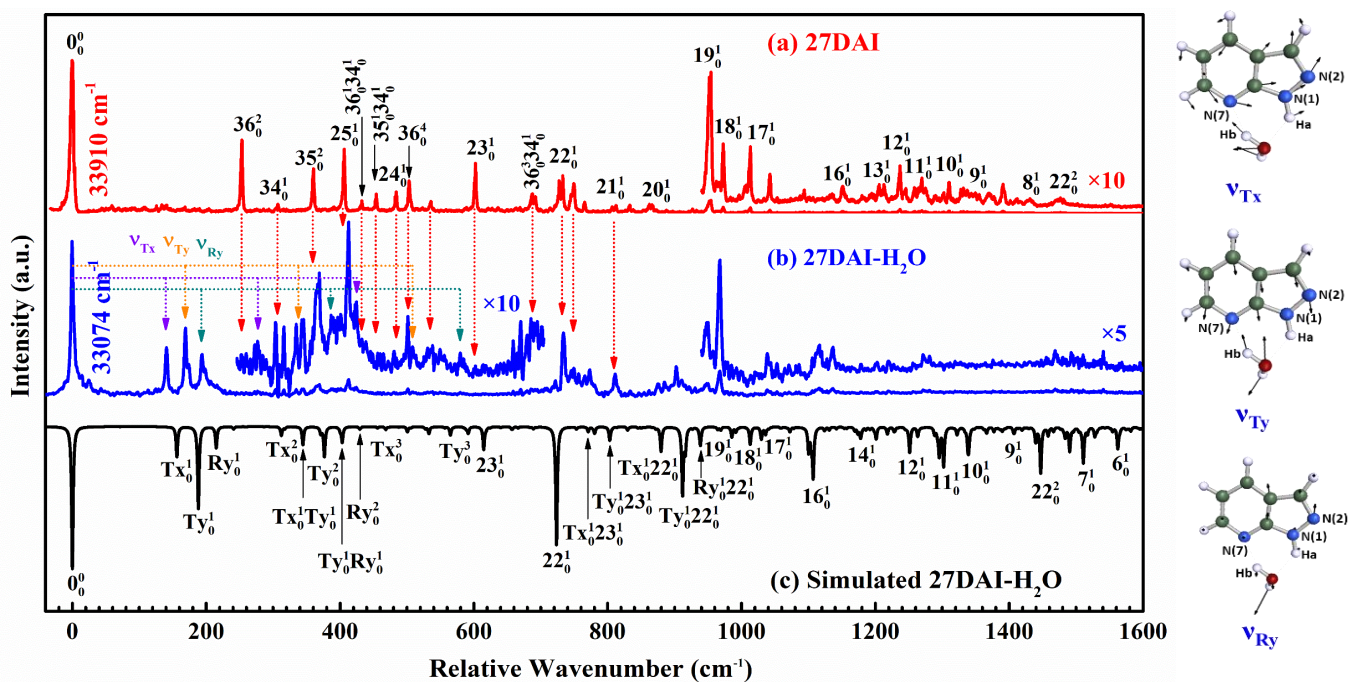


Figure 1. Two-colour resonant two-photon ionization spectra of $S_1 \leftarrow S_0$ transition in (a) 27DAI (33850-35510 cm^{-1}) and (b) 27DAI- H_2O (32950-34670 cm^{-1}) are shown. (c) The Franck-Condon vibronic spectrum of 27DAI- H_2O complex with the possible assignments, simulated at DFT-D4(B3LYP)/def2-TZVPP level of theory (black trace). The vibrational modes corresponding to internal translation and rotation of H_2O molecule along x- and y-axis with respect to 27DAI are represented on the right side.

Table S1). The comparison of the R2PI spectra of 27DAI- H_2O with that of 27DAI clearly depicted nearly similar vibrational frequencies of the intramolecular vibrational modes, as shown by the downward red arrows in Figure 1. The striking difference between the spectra is the appearance of lower energy modes at 141, 169 and 194 cm^{-1} . The above bands are the intermolecular modes originating from the internal motions of H_2O molecule in the complex. Additionally, the lower energy intramolecular asymmetric modes of 27DAI ($<800 \text{ cm}^{-1}$) have shown significantly diminished intensities in the complex. As mentioned in an earlier article, the above bands most likely appeared due to the distortion of the imidazolyl ring in the excited state.²⁸ The lowering of the Franck-Condon activity of the bands in 27DAI- H_2O complex can be linked to lower distortion of the aromatic ring in the hydrogen bonded structure.

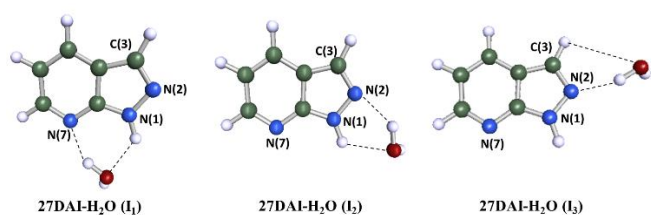


Figure 2: The possible isomers of 27DAI- H_2O in the ground state calculated at B3LYP-D4/def2-TZVPP level of theory.

3.2 Isomeric structures of 27DAI- H_2O complex

Figure 2 shows the optimized structures of 27DAI- H_2O isomers obtained using B3LYP-D4/def2-TZVPP level of theory. The zero-point vibrational energy corrected binding energies (ΔE) of the complexes are given in Table 1. The most stable structure in the ground state is the I_1 isomer, 27DAI- $\text{H}_2\text{O}(I_1)$, which shows N(1)- $\text{H}\cdots\text{O}$ and $\text{O}-\text{H}\cdots\text{N}(7)$ hydrogen bonds, with a binding energy of $-35.9 \text{ kJ mol}^{-1}$. The I_2

isomer, 27DAI- $\text{H}_2\text{O}(I_2)$, stabilized by $\text{O}-\text{H}\cdots\text{N}(2)$ hydrogen bond is the second most stable isomer with binding energy of $-25.8 \text{ kJ mol}^{-1}$. A high energy isomer, 27DAI- $\text{H}_2\text{O}(I_3)$, is also optimized with a $\text{C}(3)-\text{H}\cdots\text{O}$ hydrogen bond. The solvent molecules have shown different docking sites in the above complexes. All the structures possess hydrogen bonded OH and NH bonds, which can be detected using infrared spectroscopic schemes. For the gas phase molecular complexes, the state-of-the-art IR-UV double resonance spectroscopic techniques were employed in 3100-3550 cm^{-1} region to probe the docking sites of the solvent in the complex.

Table 1: The calculated binding energies ΔE of the complexes at B3LYP-D4/def2-TZVPP level are given. The experimental and calculated (scaled with a factor of 0.961(S_0) and 0.969(S_1)) N-H and O-H frequencies in the ground and excited state of the 27DAI- H_2O complexes are listed with total shift (Δv_{shift}).

System	ΔE (kJmol^{-1})	Calculated (cm^{-1})		
		ν_{NH}	ν_{OH}	Δv_{shift}
27DAI (S_0) (Expt)	-	3523	-	-
27DAI- H_2O (S_0) (Expt)	-	3414	3447	-319
27DAI- H_2O (I_1) (S_0)	-35.9	3397	3427	-358
27DAI- H_2O (I_2) (S_0)	-25.8	3446	3535	-200
27DAI- H_2O (I_3) (S_0)	-19.0	3523	3724	+66
27DAI (S_1) (Expt)	-	3467	-	-
27DAI- H_2O (S_1) (Expt)	-	3210	3265	-649
1H- H_2O (I_1) (S_1)	-55.3	3201	3257	-698
1H- H_2O (I_2) (S_1)	-50.1	3365	3630	-160

3.3 Structural determination: Ion-dip Infrared (IDIR) and Fluorescence-dip Infrared (FDIR) Spectroscopy

Figure 3A shows the IDIR spectrum of the jet cooled 27DAI- H_2O complex. The spectrum was recorded by scanning the IR-OPO laser, which was introduced $\sim 3 \text{ ns}$ prior to the excitation laser, fixed at the

$S_1 \leftarrow S_0$ band origin of the 27DAI-H₂O complex i.e., 33074 cm⁻¹. The ionization laser, fixed at 213 nm, is nearly overlapped with the excitation laser for the best signal-to-noise ratio of the R2PI signal. Because both the ionization laser and IR OPO were pumped by a single Nd:YAG laser, the temporal delay between the laser pulses were generated using an optical path difference. The above restricts the delay between the IR and UV (excitation) pulses to ~ 3 ns only. Due to the above, both the ground and excited state vibrational bands can be simultaneously detected in the spectrum.²⁸

The IDIR spectrum shown in Figure 3A depicts four vibrational bands at 3447, 3414, 3265 and 3210 cm⁻¹. Among them, the highest energy band is positioned at 3447 cm⁻¹. Note that, the $\nu_{\text{N-H}}$ of free 27DAI molecule²⁸ was positioned at 3523 cm⁻¹ and the two OH stretching frequencies of an isolated H₂O in the gas phase are expected at 3657 and 3756 cm⁻¹.³⁶ Therefore, the above peaks are significantly red shifted due to hydrogen bonding interaction. The simulated IR spectra of all the three isomers of 27DAI-H₂O suggested the presence of two hydrogen bonded vibrational modes in the above spectral range, i.e., hydrogen bonded N-H and O-H groups. The four experimental bands can thus represent the hydrogen bonded N-H and O-H groups in both the ground and excited states. Note that, the free O-H of the water molecule (>3600 cm⁻¹) is expected outside the range of the currently used KTP based IR-OPO output (3100-3550 cm⁻¹).

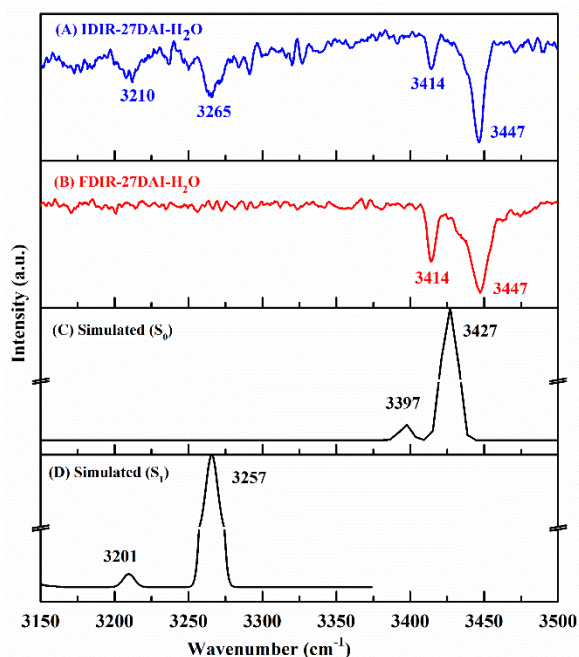


Figure 3. (A) IDIR and (B) FDIR spectra of 27DAI-H₂O complex recorded by monitoring the band at 33074 cm⁻¹. The IR-UV temporal delay in (A) and (B) are ~ 3 and 20 ns, respectively. (C) and (D) represents the calculated IR spectra (scaled using 0.961 and 0.969) in the S_0 and S_1 states, respectively.

For the unambiguous assignment of the ground and excited state vibrational bands, we have also recorded the FDIR spectrum of the complex. Here, the scanning IR laser was introduced 20 ns prior to the excitation laser (fixed at 33074 cm⁻¹) and the fluorescence dip in the spectrum was observed as a function of IR vibrational frequency. Note that, the temporal delay between the IR and excitation lasers can be varied using a digital delay generator as both the IR and UV lasers are pumped by separate Nd:YAG lasers. At the higher delay, only the ground state can be depopulated using the IR laser. The subsequent excitation laser can only excite the depopulated ground

state to provide the fluorescence depletion. The above set-up thus prevented any depopulation of the excited molecule. Figure 4B (red trace) shows the FDIR spectrum containing only two bands in the spectral range at 3447 and 3414 cm⁻¹. Both the bands were also detected using IDIR spectroscopy (Figure 3A). The bands thus belong to the ground state frequencies of the complex. The bands absent in the FDIR spectrum, i.e., the bands at 3210 and 3265 cm⁻¹ represent the corresponding vibrational frequencies of 27DAI-H₂O complex in the S_1 state.

The calculated vibrational frequencies (given in Table 1, scaled using 0.961) of hydrogen bonded ν_{NH} and ν_{OH} frequencies of I_1 , I_2 and I_3 isomers of 27DAI-H₂O complex are shown in Table 1. In the case of 27DAI-H₂O(I_1), the hydrogen bonded ν_{NH} and ν_{OH} bands were identified at 3397 and 3427 cm⁻¹, respectively, which are detected at 3414 and 3447 cm⁻¹, respectively. The combined calculated shift of the hydrogen bonded $\nu_{\text{N-H}}$ and $\nu_{\text{O-H}}$ modes in the complex is -358 cm⁻¹ has shown a good agreement with the experimental combined shift of -319 cm⁻¹. The combined shifts are calculated as: $\Delta\nu_{\text{shift}} = [\nu_{\text{NH}}(27\text{DAI-H}_2\text{O}) - \nu_{\text{NH}}(27\text{DAI})] + [\nu_{\text{OH}}(27\text{DAI-H}_2\text{O}) - \nu_{\text{OH}}(\text{H}_2\text{O})]$. The calculated combined shift at -200 in I_2 and +66 in isomer I_3 highly differ from the experimental value of -319 cm⁻¹. Therefore, the experimental data matches well with the I_1 isomer of 27DAI-H₂O complex. In the case of 7AI-H₂O complex,³⁶ the ν_{NH} was reported at 3412 cm⁻¹ which is similar to that of 27DAI-H₂O complex (3414 cm⁻¹). However, the ν_{OH} of 7AI-H₂O complex was reported at 3369 cm⁻¹, which is much lower than the 3447 cm⁻¹ band in 27DAI-H₂O complex. This is most likely due to the higher binding energy 7AI-H₂O at -39.9 kJmol⁻¹ than that of 27DAI-H₂O complex (-35.9 kJmol⁻¹) at B3LYP-D4/def2-TZVPP level of theory. The above is also reflected in the bond lengths data where $R_{\text{N(1)-H}_a}$ remains same for both 7AI-H₂O (1.012 Å) and 27DAI-H₂O (1.013 Å), however, the $R_{\text{N(7)-H}_b}$ is much lower for 7AI-H₂O (1.809) than 27DAI-H₂O (1.856) complex in the ground state (SI Table S1). This suggests that the N(2) in case of 27DAI-H₂O complex has an overall electron-withdrawing effect on N(7) group which reduces the basicity at N(7) compared to that in 7AI-H₂O complex.

The IDIR bands at 3210 and 3265 cm⁻¹ were only detected when the IR laser is partially overlapped with the excitation laser, as the relative delay is only ~ 3 ns. In this, the population of the vibrationless S_1 state can also be depleted by the resonant IR transition in addition to the ground state. Therefore, the above two bands belong to the excited state of the 27DAI-H₂O(I_1) complex. Similar observations are recently reported for 27DAI in the gas phase where the excited state N-H frequency was significantly red shifted at 3467 cm⁻¹ compared to that of 7AI monomer (3489 cm⁻¹). The above indicates the comparatively higher photo acidity of N(1)-H_a in N(2) substituted 27DAI.^{28,37} Further, we have compared the calculated IR spectrum of the molecule in the excited S_1 state. Figure 3D clearly depicts two vibrational modes at 3257 and 3210 cm⁻¹ (Table 1). The band positions agree excellently with our experimentally obtained vibrational frequencies, confirming the origin of the two bands to the excited state of the molecular complex. The experimental bands at 3265 and 3210 cm⁻¹ are affirmatively assigned to the hydrogen bonded ν_{OH} of the H₂O and ν_{NH} of the 27DAI of the complex. The combined shift of the vibrations measure experimentally is 649 cm⁻¹ which matches well with the calculated combined shift of 698 cm⁻¹. The structure of complex is therefore confirmed to be 27DAI-H₂O(I_1) in the ground and excited states.

For the simplicity, the name '27DAI-H₂O' is used for the rest of the discussion referring to the I_1 isomer of the complex (Figure 2). Moreover, the excited state N-H frequency of the 27DAI-H₂O complex is found to have lower than that in the ground state which manifests the increased photo acidity of the water complex in the

excited state. Further, N-H frequencies of the 27DAI-H₂O complex in both ground and excited states are lower than the 27DAI monomer, suggesting the enhanced feasibility of the excited state photochemical processes on micro solvation.

Table 2: The experimental band positions and the corresponding vibrational frequencies ν' in the S_1 state of the 27DAI-H₂O complex are listed with the possible assignments. The calculated excited state (S_1) frequencies (scaling factor 0.954) and the ν' values of 27DAI are mentioned for comparison. The numbers in bold represent the totally symmetric vibrational modes.

27DAI-H ₂ O				27DAI
Position	ν'_{expt}	ν'_{calc}	Assign.	ν'_{expt}
33074	0	0	0_0^0	0
33215	141	156	Tx_0^1	-
33243	169	188	Ty_0^1	-
33268	194	215	Ry_0^1	-
33350	276	312	Tx_0^2	-
33378	304	-	34_0^1	307
33388	314	344	$\text{Tx}_0^1\text{Ty}_0^1$	-
33419	345	376	Ty_0^2	-
33442	368	403	$\text{Ty}_0^1\text{Ry}_0^1$	-
33461	387	430	Ry_0^2	-
33486	412	400	25_0^1	406
33497	423	468	Tx_0^3	-
33554	480	507	24_0^1	483
33575	501	-	36_0^4	504
33581	507	564	Ty_0^3	-
33653	579	645	Ry_0^3	-
33677	603	615	23_0^1	604
33759	685	-	$36_0^3 34_0^1$	691
33808	734	723	22_0^1	733
33823	749	771	$\text{Tx}_0^1 23_0^1$	-
33847	773	803	$\text{Ty}_0^1 23_0^1$	-
33949	875	916	20_0^1	866
33958	884	879	$\text{Tx}_0^1 22_0^1$	-
33977	903	912	$\text{Ty}_0^1 22_0^1$	-
33985	911	938	$\text{Ry}_0^1 22_0^1$	-
34022	948	985	19_0^1	957
34042	968	1013	18_0^1	975
34112	1038	1030	17_0^1	1014
34201	1127	1107	16_0^1	1153
34276	1202	1178	14_0^1	-
34351	1277	1251	12_0^1	1239
34393	1319	1302	11_0^1	1271
34435	1361	1340	10_0^1	1311
34449	1375	1377	9_0^1	1341
34542	1468	1447	22_0^2	1480
34616	1542	1511	7_0^1	-
34642	1568	1562	6_0^1	-

3.4 IR-UV hole burning experiment

IR-UV hole-burning experiment was performed while fixing the IR laser at the ground state O-H frequency at 3447 cm⁻¹ of the 27DAI-H₂O complex. The LIF spectrum was recorded with and without the IR laser, under identical experimental conditions. All the unique bands belonging to the 27DAI-H₂O complex were found to show depleted band intensities in the presence of IR laser when compared to the same scan recorded without the IR laser. Two major clusters of high intensity water bands were observed in the range 0-200 cm⁻¹

and 710-820 cm⁻¹ as shown in Figure 4a and 4b respectively. All the bands belonging to the same ground state of the complex in both the regions have shown >90% burn in their band intensities. This confirms that all the vibrational bands reported in the spectra belong to the 27DAI-H₂O complex only.

3.5 Electronic Spectroscopy: Franck-Condon Analysis

Table 2 lists the experimental bands and the corresponding vibrational frequencies of the complex in the S_1 state obtained from the R2PI spectrum of the 27DAI-H₂O complex. As shown in the structure, the hydrogen bonding between the 27DAI and water molecule did not alter the planarity of the C_s-symmetric monomer in the complex. Because of the above reason, the notations of the intramolecular bands are kept unchanged to that of the bare molecule. The Franck-Condon (FC) analysis was performed using the frequency outputs of the S_0 and S_1 states of the optimized 27DAI-H₂O complex. The simulated spectrum, scaled with a factor of 0.954, is shown in Figure 1(c), which shows a good agreement in terms of the band positions. The long FC activity (0 +1600 cm⁻¹) observed in the 27DAI-H₂O spectrum is well supplemented by the higher energy bands observed in the simulated spectra. As shown in Figure 1(C), most of the symmetric modes in the R2PI spectrum of 27DAI monomer were observed in that of the 27DAI-H₂O complex. As shown in Table 2, the intramolecular symmetric modes ν'_{25} , ν'_{24} , ν'_{23} and ν'_{22} , are positioned at 412, 480, 603 and 734 cm⁻¹, respectively. The bands are found to be marginally shifted compared to 27DAI monomer, even though the intensities of the transitions are significantly diminished. The corresponding bands in 27DAI monomer were positioned at 406, 483, 604 and 733 cm⁻¹, respectively, which are nearly unchanged upon complex formation (Figure 1).

The R2PI spectrum has shown the intermolecular modes at 141 (ν'_{Tx}), 169 (ν'_{Ty}) and 194 (ν'_{Ry}) cm⁻¹. The ν_{Tx} and ν_{Ty} modes are the intermolecular modes associated with the internal translational motions of the H₂O molecule with respect to the 27DAI along the x- and y-axes, respectively. The ν_{Ry} represents the internal rotational motion of the H₂O molecule with respect to the y-axis of the 27DAI-H₂O complex.³⁰ Similar vibrational modes were also observed for the 7AI-H₂O complex. The progressions of the above modes were also observed at 276 (2 ν'_{Tx}) and 423 (3 ν'_{Tx}), 345 (2 ν'_{Ty}) and 507 (3 ν'_{Ty}), and 387 (2 ν'_{Ry}) and 579 (3 ν'_{Ry}) cm⁻¹, in addition, the combination

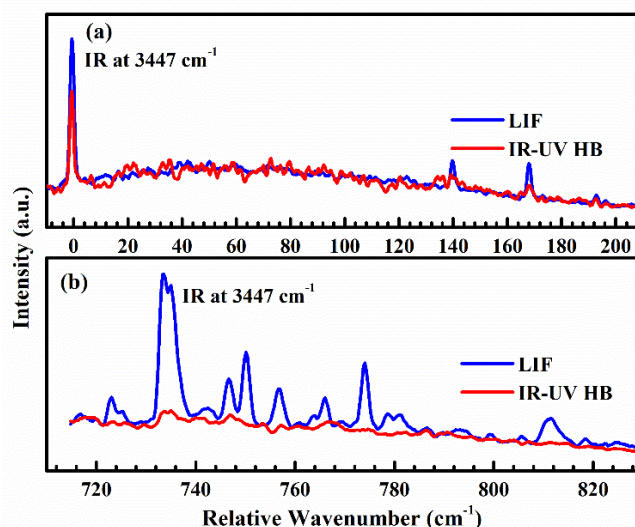


Figure 4. IR-UV hole burning spectrum (red trace) recorded at ν_{IR} of 3447 cm⁻¹. The LIF spectrum in blue trace is shown for comparison.

bands are also observed at 314 ($\nu''_{\text{Tx}}\nu''_{\text{Ty}}$) and 368 ($\nu''_{\text{Ty}}\nu''_{\text{Ry}}$) cm^{-1} . Further, the combination bands of the above intermolecular modes with the symmetric modes are also observed at 749 ($\nu''_{\text{Tx}}\nu''_{23}$), 773 ($\nu''_{\text{Ty}}\nu''_{23}$), 884 ($\nu''_{\text{Tx}}\nu''_{22}$), 903 ($\nu''_{\text{Ty}}\nu''_{22}$) and 911 ($\nu''_{\text{Ry}}\nu''_{22}$) cm^{-1} . The higher energy vibrational modes ν''_{16} at 1027 cm^{-1} , have shown - 26 cm^{-1} of redshift in the complex. However, several modes, such as ν''_{20} , ν''_{17} , ν''_{11} , ν''_{10} , ν''_9 have shown blue shifted transitions. The above spectral shifts are in agreement with the assigned structures, as the calculated vibrational frequencies predicted the above bands reasonably well. Additionally, the intensities of all the above lower energy bands were significantly diminished in the water complex, except the ν''_{22} mode. The lower intensity of the intramolecular asymmetric modes $2\nu''_{36}$, ν''_{34} , $2\nu''_{35}$, $\nu''_{36}\nu''_{34}$, $\nu''_{35}\nu''_{34}$ and the higher energy combination bands could be linked to the formation of the hydrogen bonded complex. It is worth to mention that; the asymmetric bands were important to characterize the structure of the 27DAI molecule in the excited state.²⁸ The transitions above 1000 cm^{-1} from the origin band are significant weak compared to the lower energy modes, similar to 27DAI monomer. This is most likely due to the lower excited vibrational state lifetime. However, the bands were detected till 1600 cm^{-1} above the band origin transitions, as shown in Figure 1.

3.6 Single vibronic level fluorescence (SVLF) spectroscopy

Figure 5 represents the SVLF spectrum of 27DAI-H₂O complex obtained from exciting at the origin band (0_0^0) positioned at 33074 cm^{-1} . The ground state vibrational modes are detected till 3000 cm^{-1} . The positions of the ground state vibrational bands along their possible assignments based on the Franck-Condon simulation are given in Table 3. Similar to the 2C-R2PI spectrum, the three prominent intermolecular modes were detected at 115 (ν''_{Tx}), 152 (ν''_{Ty}) and 190 (ν''_{Ry}) cm^{-1} . The above internal translational modes are detected at 141 (ν''_{Tx}) and 169 (ν''_{Ty}) in the S_1 state, which have shown significantly blue shift upon electronic transitions. As mentioned earlier, the binding energy of the complex is more negative in the S_1 state of the complex, the corresponding hydrogen bond energies must be higher. Therefore, the increase in ν''_{Tx} and ν''_{Ty} modes is in line to the increase in hydrogen bond interaction energies. The progressions of the above modes were also observed at 234 ($2\nu''_{\text{Tx}}$), 298 ($2\nu''_{\text{Ty}}$), 338 ($3\nu''_{\text{Tx}}$) and 357 ($2\nu''_{\text{Ry}}$) cm^{-1} . Further, the combination bands of the above modes with the symmetric modes are also observed at 874 ($\nu''_{\text{Tx}}\nu''_{22}$), 909 ($\nu''_{\text{Ty}}\nu''_{22}$) and 929 ($\nu''_{\text{Ry}}\nu''_{22}$) cm^{-1} . The SVLF spectra of the 27DAI is shown in Figure 5 and the band positions of the monomer are given in Table 3, for comparison. Most the symmetric modes of 27DAI are seen in the 27DAI-H₂O complex. The ground vibrational frequencies in the complex are observed within 15 cm^{-1} of the excited state values, (except ν''_{20}). The transition at 759 cm^{-1} is found to be the strongest transition among all the symmetric modes, similar to the SVLF spectrum of 27DAI monomer. A progression of the above mode has been observed till $3\nu''_{22}$. In the excitation spectrum of 7AI and 7AI-H₂O cluster, the above mode was observed to be the strongest mode, similar of 27DAI.³³ All the experimentally detected vibrational modes are found to be in good agreement with the modes obtained from the Franck-Condon simulated spectra (SI Figure S1).

3.7 Photoionization efficiency spectroscopy

The ionization energy of a molecular complex is directly linked to its photostability. The 27DAI molecule (8.921 eV)²⁸ has shown significantly higher ionization energy compared to the N-less counterparts, such as 7-azaindole (8.11 eV) and Indole (7.76 eV), as reported earlier.³⁸⁻⁴¹ Additionally, the 2C-R2PI spectroscopy required appropriate photon energy to generate ion signal. The $S_1 \leftarrow S_0$ band

origin transition of 27DAI-H₂O at 33074 cm^{-1} , accounts for 4.100 eV of energy. The 4th-harmonic of Nd:YAG laser at 266 nm (4.661 eV) **Table 3: The experimental band positions and the corresponding vibrational frequencies in the ground state ν'' of the 27DAI-H₂O are listed with the possible assignments. The calculated excited state (S_1) frequencies (scaling factor 0.973) and the ν' values of 27DAI are mentioned for comparison. The numbers in bold represent the totally symmetric vibrational modes.**

27DAI-H ₂ O				27DAI
Position	ν''_{expt}	ν''_{calc}	Assign.	ν''_{expt}
33074	0	0	0_0^0	
33189	115	119	Tx_1^0	-
33226	152	162	Ty_1^0	-
33264	190	199	Ry_1^0	-
33308	234	238	Tx_2^0	-
33372	298	324	Ty_2^0	-
33412	338	357	Tx_3^0	-
33431	357	398	Ry_2^0	-
33501	427	426	25_1^0	426
33616	542	552	24_1^0	552
33701	627	633	23_1^0	642
33833	759	770	22_1^0	769
33888	814	878	34_2^0	848
33948	874	889	$\text{Tx}_1^0 22_1^0$	-
33983	909	932	$\text{Ty}_1^0 22_1^0$	-
34003	929	969	$\text{Ry}_1^0 22_1^0$	-
34043	969	935	20_1^0	939
34096	1022	1030	19_1^0	1035
34140	1066	1072	18_1^0	1087
34183	1109	1103	24_2^0	1120
34289	1215	1201	16_1^0	1214
34354	1280	1311	13_1^0	1294
34379	1305	1319	12_1^0	1313
34464	1390	1410	10_1^0	1405
34596	1522	1540	22_2^0	1537
34674	1600	1601	6_1^0	1607
34910	1836	1870	20_2^0	1853
35122	2048	2060	19_2^0	2067
35212	2138	2144	18_2^0	2162
35367	2294	2310	22_3^0	2293

was insufficient to generate any resonant ion signal from the 27DAI-H₂O complex at a combined energy of 8.761 eV. The ionization energy of the 27DAI-H₂O complex was calculated as 8.470 eV at B3LYP-D4/def2-TZVPP level of theory. To find the ionization energy of the complex, we recorded the photoionization spectra of the molecular complex UV-UV pump-probe technique. The excitation laser (pump) was fixed at 4.100 eV (band origin of the complex) and a second scanning UV laser was used to probe the ionization threshold of the complex. The spectrum is shown in Figure 6 and the ionization energy was determined at 8.789±0.001 eV from the recorded PIE spectrum. The ion signal was found to be significantly stronger in the region 8.95-9.20 eV. The ionization energy obtained for 27DAI-H₂O complex was lower by 0.132 eV (1065 cm^{-1}) than the 27DAI monomer, suggesting the increased stabilization of the ionic state upon solvation. Similar observation is also seen in case of 7AI-H₂O complex. In that case, the IE of the complex is reported at

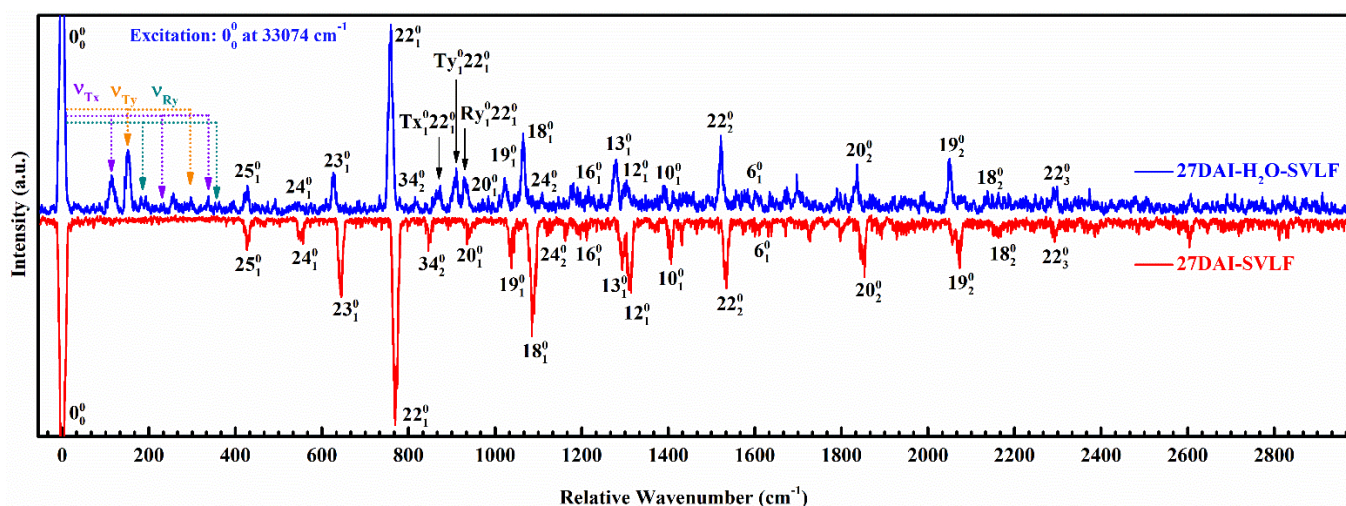


Figure 5. Single vibronic level fluorescence (SVLF) spectrum of 27DAI-H₂O (blue trace) recorded by exciting at the origin band positioned at 33074 cm⁻¹. The inverted spectrum shows the S₀←S₁ transitions of 27DAI monomer with assignments (red trace)

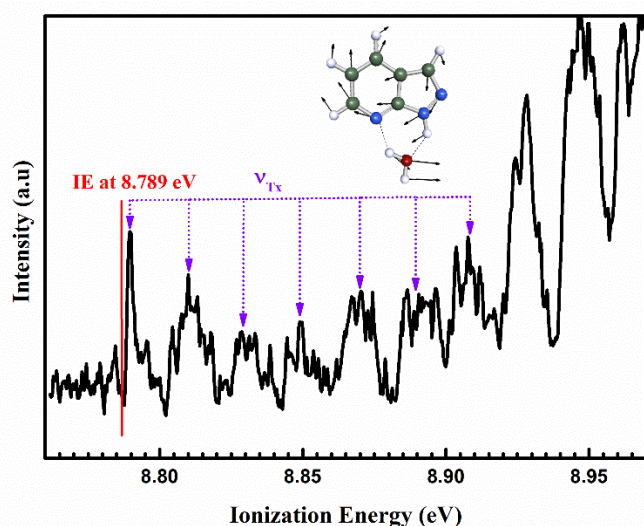


Figure 6. The photoionization efficiency (PIE) spectrum of 27DAI-H₂O complex was recorded by keeping the excitation laser fixed at the band origin at 33074 cm⁻¹ (4.100 eV). The X-axis represents combined energy of excitation and ionization energy in eV. (8.789 eV)

7.933±0.003 eV which is lower by 0.177 eV (1428 cm⁻¹) in comparison to bare 7AI (8.11 eV).^{39,41} (SI Figure S3). Additionally, the IE of 27DAI-H₂O complex is significantly higher than that of 7AI-H₂O complex. Further, the progression of 169 cm⁻¹ is observed in the photoionization spectrum which corresponds to the ν_{Tx} mode at 189 cm⁻¹ for the cationic species of 27DAI-H₂O calculated at B3LYP-D4/def2-TZVPP level of theory.

3.8 27DAI-(H₂O)₂ complex

The LIF spectrum of the 27DAI in the presence of water vapour under appropriate conditions displays additional bands in 32500-33000 cm⁻¹ region, as shown in Figure 7. Note that, the dye laser output in the region 615-600 nm (32500-33000 cm⁻¹) region was quite challenging because of the unavailability of appropriate commercially available laser dyes. We mixed DCM and Rhodamine-6G laser dyes in ethanol to use as the dye solution and pumped the dye laser using 532 nm out-put of Nd:YAG laser (SHG). The above generated sufficient lasing

for the measurement of LIF spectrum (Figure 7 bottom spectrum). The strongest transition was observed at 32565 cm⁻¹. The spectrum is most likely generated from the 27DAI-(H₂O)₂ complex. The R2PI spectrum at 27DAI-(H₂O)₂⁺ ion signal could not be recorded due to low ion signal-to-noise at the region due to low laser power. The band at 32565 cm⁻¹ is red shifted by 1345 cm⁻¹ compared to the origin band of 27DAI molecule. The above large redshift is commensurate with the higher solvent cluster of 27DAI. A similar large redshift was also observed for 7AI-(H₂O)₂ complex.³³ Further analysis was performed to investigate the molecular source of the band at 32565 cm⁻¹.

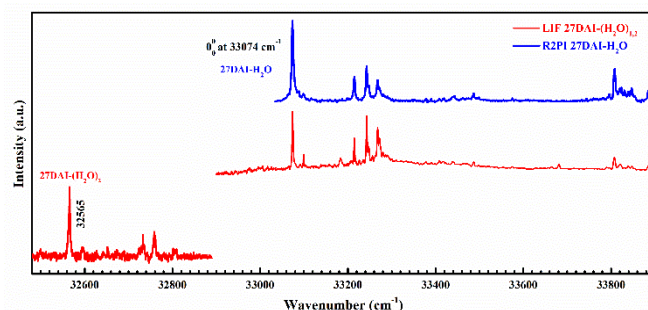


Figure 7. LIF spectrum of 27DAI-(H₂O)_{1,2} is shown at the bottom (red traces) along with the R2PI spectrum of 27DAI-H₂O (blue trace). The bands in 32500-33000 cm⁻¹ region belong to two water clusters.

Fluorescence dip-infrared (FDIR) spectroscopy provides the ground state vibrational frequencies of the complex associated to the above-mentioned band at 32565 cm⁻¹. The scanning IR laser (3100-3550 cm⁻¹) was introduced 20 ns prior to the excitation laser and the fluorescence dip in the spectrum was obtained as function of IR vibrational frequency. Due to the larger delay, only the ground state could be depopulated using the IR laser. The measured FDIR spectrum of the band is shown in Figure 8(A). The FDIR spectrum has shown broader peaks suggesting a swallow potential of the complex along the N-H and O-H vibrational coordinate in the complex. A three peak fitting was done as the water dimer is expected to show one NH, two hydrogen bonded O-H bands in the above spectral region. The fit shows good agreement with the observed spectrum with band centres positioned at 3207, 3261 and 3385 cm⁻¹. Note that, the

free O-H groups are expected to be above 3600 cm^{-1} , as reported in previous studies of $7\text{AI}-(\text{H}_2\text{O})_2$ complexes.³⁶

Figure 9 shows the optimized structures of $27\text{DAI}-(\text{H}_2\text{O})_2$ isomers obtained using B3LYP-D4/def2-TZVPP level of theory. The zero-point vibrational energy corrected binding energies of the possible

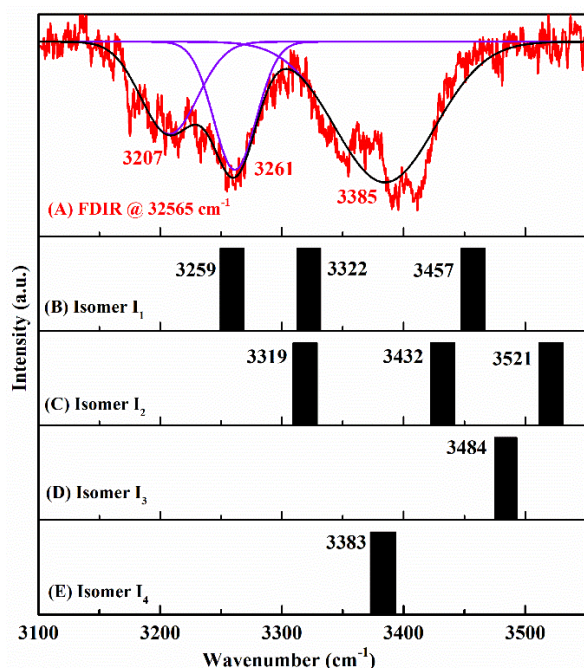


Figure 8: (A) FDIR spectrum of $27\text{DAI}-(\text{H}_2\text{O})_2$ recorded by monitoring the band of the complex at 32565 cm^{-1} . The IR-UV temporal delay in (A) is 20 ns. (B)-(E) represents the simulated IR spectra of various isomers.

complexes are given in Table 4. The most stable ground structure is the isomer $27\text{DAI}-(\text{H}_2\text{O})_2(\text{I}_1)$, which shows $\text{N}(1)-\text{H}\cdots\text{O}$ and $\text{O}-\text{H}\cdots\text{N}(7)$ hydrogen bonds between the molecules, similar to that in one water complex $27\text{DAI}-\text{H}_2\text{O}(\text{I}_1)$. The binding energy of the following complex was obtained as -80.0 kJ mol^{-1} . The I_2 isomer $27\text{DAI}-(\text{H}_2\text{O})_2(\text{I}_2)$, stabilized by $\text{N}(1)-\text{H}\cdots\text{O}$ and $\text{O}-\text{H}\cdots\text{N}(2)$ hydrogen bonds, is the second most stable isomer with binding energy of -70.8 kJ mol^{-1} . Two other high energy isomers, $27\text{DAI}-(\text{H}_2\text{O})_2(\text{I}_3)$ (-52.7 kJ mol^{-1}) and $27\text{DAI}-(\text{H}_2\text{O})_2(\text{I}_4)$ (-54.2 kJ mol^{-1}) are optimized with $\text{C}-\text{H}\cdots\text{O}$ and $\text{N}\cdots\text{O}-\text{H}$ hydrogen bonds. In the structures, the solvent molecules have shown different docking sites. Isomers I_1 and I_2 have shown three relatively stronger hydrogen bonded groups, N-H of the chromophore and two O-H from the two solvent molecules. The above two complexes are highly likely to be the origin of the $\text{DAI}-(\text{H}_2\text{O})_2$ band systems. Note that, the lower energy isomers do not show any hydrogen bonded N-H and only two hydrogen bonded O-H bonds are expected to be identified in the mentioned spectral region. The vibrational frequencies of the hydrogen bonded N-H and O-H frequencies are shown in Table 4 along with the experimental values.

To gain further support toward the structural assignment, we have compared the calculated frequencies of $27\text{DAI}-(\text{H}_2\text{O})_2$ isomers in Figure 8. The calculated vibrational frequencies of the hydrogen bonded N-H (3259 cm^{-1}) and O-H groups (3322 and 3457 cm^{-1}) of I_1 isomer were excellently correlated (SI Figure S2) with the experimental values of 3207 , 3261 and 3385 cm^{-1} , respectively. The correlation factor in SI Figure S2 for I_1 isomer was obtained as 0.982 with residual sum of squares (RSS) as low as 138 cm^2 . The next best correlation was observed for I_2 isomer with the RSS value of 1702 cm^2 , which was higher by an order of magnitude. Considering the higher binding energy of I_1 structure, better correlation with the

experimental values, the structure of $27\text{DAI}-(\text{H}_2\text{O})_2$ for the band at 32565 cm^{-1} can be assigned to the isomer I_1 (Figure 9). In the case of $7\text{AI}-\text{H}_2\text{O}$ complex, the ν_{NH} is reported at 3112 cm^{-1} and the ν_{OH} values are obtained at 3200 , 3251 , 3301 and 3341 cm^{-1} .³⁶

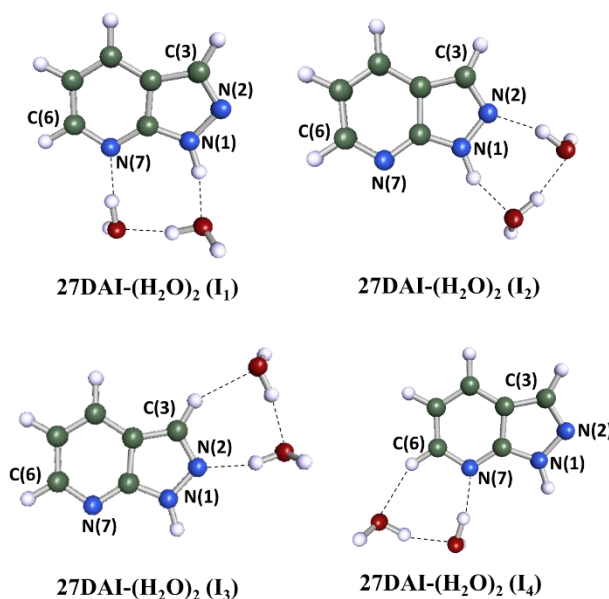


Figure 9. The possible isomers of $27\text{DAI}-(\text{H}_2\text{O})_2$ in the ground state calculated at B3LYP-D4/def2-TZVPP level of theory.

Table 4: The experimental N-H and hydrogen bonded O-H frequencies in in the ground state of the $27\text{DAI}-(\text{H}_2\text{O})_2$ complex obtained from FDIR spectrum along with the calculated vibrational frequencies for all the possible isomers. The calculated vibrational frequencies are unscaled. The calculated binding energies of the isomeric complexes at B3LYP-D4/def2-TZVPP level of theory are also given.

Systems	ΔE (kJ mol^{-1})	Frequency (cm^{-1})		
		ν_{NH}	ν_{OH}	ν_{OH}
27DAI (Expt)	-	3523	-	-
27DAI-(H₂O)₂ (Expt)		3207	3385	3261
27DAI-(H₂O)₂ (I₁)	-80.0	3259	3457	3322
27DAI-(H₂O)₂ (I₂)	-70.8	3319	3521	3432
27DAI-(H₂O)₂ (I₃)	-52.7	3668	3575	3484
27DAI-(H₂O)₂ (I₄)	-54.2	3664	3573	3383

Overall, the structure of $27\text{DAI}-\text{H}_2\text{O}$ and $27\text{DAI}-(\text{H}_2\text{O})_2$ have shown one- and two-solvent bridges between the $\text{N}(1)\text{H}$ and $\text{N}(7)$ groups of 27DAI molecule, respectively. Note that, the above structural configurations were reported to be ideal for efficient excited state hydrogen transfer process in the molecule. The larger solvent chain can decrease the energy barriers for the hydrogen transfer reaction in the excited state. The current set of data can thus be considered a stepping stone to investigate the photoinduced tautomerization of N-bearing biologically relevant molecules.

3.9 Correlation of the experimental and calculated frequencies:

Figure 10 shows the correlation between the calculated vibrational frequencies of both 27DAI and $27\text{DAI}-\text{H}_2\text{O}$ at B3LYP-D4/def2-TZVPP (ground state S_0) and TD-B3LYP-D4/def2-TZVPP (excited state S_1) levels of theories with the corresponding bands obtained from the SVLF and R2PI spectroscopies, respectively. Here, only the totally symmetric modes were used for the analysis. Both graphs have

shown excellent correlations between the data. The linear fit functions shown in the figure shows the factors of 0.973 ± 0.002 for the ground and 0.954 ± 0.004 for the excited state to obtain the experimental values. The actual residuals, shown for each set of data suggest a better correlation for the ground state vibrations than that for the excited state values. Considering only the 27DAI data, the above factors are 0.971 ± 0.002 and 0.950 ± 0.005 , which are within the tolerance limit of the linear fit functions. The above suggests the robustness of the computational method used here, in terms of the prediction of the hydrogen bonded clusters of 27DAI in both the ground and excited states. Additionally, based on the ν_{NH} stretching frequencies of 27DAI, the factors obtained for $3100\text{--}3500\text{ cm}^{-1}$ are 0.961 in S_0 state and 0.969 in the S_1 state. Both factors provide excellent correlation to predict the hydrogen bonded NH and OH vibrational frequencies in the ground and excited states. The above factors are noticeably lower in S_0 and higher in S_1 states for the frequencies $<1600\text{ cm}^{-1}$. Therefore, the factors used to scale the Franck-Condon simulation spectrum, the scaling factors, were used from the correlation fit shown in Figure 10. However, the ν_{NH} and ν_{OH} stretching frequencies are scaled using the factors obtained using the experimental and calculated ν_{NH} of the 27DAI monomer.

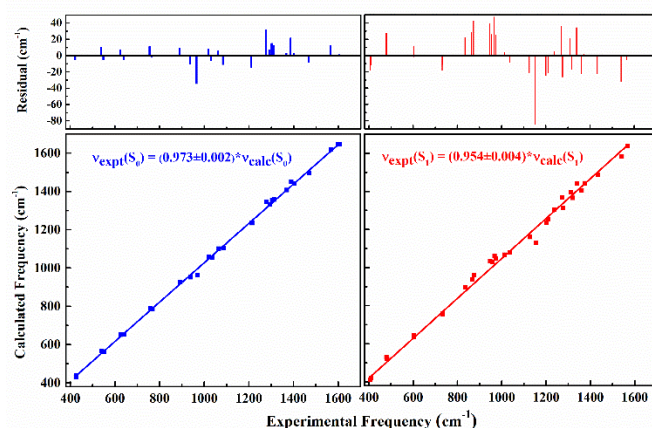


Figure 10. Correlation between the experimental and calculated totally symmetric modes of 27DAI and 27DAI-H₂O systems obtained for the ground (S_0) and excited (S_1) states. The top shows the residual of the datapoint post linear fit. The correlation factors in the ground and excited states are given.

4 Conclusion

In this article, we have investigated the 1:1 and 1:2 complexes of 27DAI with H₂O to understand the hydrogen bonding interaction in the complexes in the ground and excited states. The $S_1 \leftarrow S_0$ excitation spectrum was recorded using R2PI technique and the electronic transition (0_0^0) of 27DAI-H₂O complex appeared at 33074 cm^{-1} . The band origin was red shifted by 836 cm^{-1} compared to that of bare 27DAI. The R2PI spectrum shows the appearance of unique lower energy intermolecular modes at 141 , 169 and 194 cm^{-1} , originating from the internal motions of H₂O molecule in the complex. The IR-UV hole burning spectroscopy confirmed the presence of only one isomer in the molecular beam, i.e., 27DAI-H₂O(I_1). To investigate the most preferred docking side of the 27DAI-H₂O complex, we have employed Ion-dip Infrared (IDIR) and Fluorescence-dip Infrared (FDIR) spectroscopy. The ground state hydrogen bonded $\nu_{\text{N-H}}$ and $\nu_{\text{O-H}}$ frequencies were observed at 3414 and 3447 cm^{-1} , respectively. In the excited state, the hydrogen bonded $\nu_{\text{N-H}}$ and $\nu_{\text{O-H}}$ frequencies of

27DAI-H₂O are observed at 3210 and 3265 cm^{-1} which are in good agreement with the calculated values of 27DAI-H₂O(I_1), respectively. The combined experimental shifts at -319 in S_0 and -649 cm^{-1} in S_1 have shown excellent correlation with that calculated at -358 cm^{-1} and -698 cm^{-1} , respectively for the structure 27DAI-H₂O(I_1).

The ground state vibrational modes were detected till 3000 cm^{-1} in the SVLF spectrum of the 27DAI-H₂O complex. Similar to the R2PI spectrum, the three prominent intermolecular modes were detected at 115 (ν''_{Tx}), 152 (ν''_{Ty}) and 190 (ν''_{Ry}) cm^{-1} . The modes were blue shifted upon electronic excitation, suggesting a stronger hydrogen bonding interaction in the photo-excited state.

The ionization energy (IE) of the 27DAI-H₂O complex was obtained as $8.789\pm 0.001\text{ eV}$, somewhat lower than the IE of the 27DAI monomer (8.921 eV). However, the above value is significantly higher than the reported IE for 7AI-H₂O complex ($7.933\pm 0.003\text{ eV}$), suggesting the higher photostability of the solvated ionic complex in case of N(2) substituted 27DAI. The progression of 169 cm^{-1} is observed in the PIE spectrum which corresponds to the ν_{Tx} mode at 189 cm^{-1} for the cationic species of 27DAI-H₂O calculated at B3LYP-D4/def2-TZVPP level of theory. To search for 1:2 complex of 27DAI-H₂O, we recorded the LIF spectrum of the 27DAI in the presence of water vapour under appropriate conditions in the red energy region, which showed additional bands in the range of $32500\text{--}33000\text{ cm}^{-1}$. The strongest transition was observed at 32565 cm^{-1} , which was originated from the 27DAI-(H₂O)₂ complex. The FDIR spectrum recorded at 32565 cm^{-1} shows the presence of three broader bands at 3207 , 3261 and 3385 cm^{-1} . The above values are in agreement with the calculated band positions of 27DAI-(H₂O)₂(I_1) complex in the ground state. The combined experimental and theoretical results of 27DAI-H₂O and 27DAI-(H₂O)₂ have shown formation of cyclic hydrogen bonded solvent bridges between the N(1)-H and N(7) groups of 27DAI molecule. The results obtained in the current study clearly indicate that 27DAI could be a potential candidate for studying excited state proton/hydrogen atom transfer reaction in the gas phase through cooperative effect of solvents such as H₂O.

Supporting information available:

The simulated spectra for dispersed fluorescence, binding energy values and correlation plots are given.

Author Contributions

SB and BK performed the experiments. SB did the computational work. SB and SM analysed the data and prepared the manuscript.

Conflicts of interest

There are no conflicts to declare.

Acknowledgements

This work has been supported by the Department of Chemistry, IIT Hyderabad and MHRD, the Government of India. SB thanks MoE for the research fellowship. BK thank UGC for the research fellowship. SM expresses sincere gratitude towards Prof. Samuel Leutwyler, the University of Bern, for his generous instrumentation aid to IITH for the experimental set-up. SM thanks SERB, DST government of India (Grant no. CRG/2019/003335) for funding.

References:

- 1 J.-M. L. Pecourt, J. Peon and B. Kohler, DNA Excited-State

- Dynamics: Ultrafast Internal Conversion and Vibrational Cooling in a Series of Nucleosides, *J. Am. Chem. Soc.*, 2001, **123**, 10370–10378.
- 2 W. J. Schreier, P. Gilch and W. Zinth, Early Events of DNA Photodamage, *Annu. Rev. Phys. Chem.*, 2015, **66**, 497–519.
- 3 S. Felicetti, J. Fregoni, T. Schnappinger, S. Reiter, R. De Vivie-Riedle and J. Feist, Photoprotecting Uracil by Coupling with Lossy Nanocavities, *J. Phys. Chem. Lett.*, 2020, **11**, 8810–8818.
- 4 M. Barbatti, A. J. A. Aquino, J. J. Szymczak, D. Nachtigallová, P. Hobza and H. Lischka, Relaxation mechanisms of UV-photoexcited DNA and RNA nucleobases, *Proc. Natl. Acad. Sci. U.S.A.*, 2010, **107**, 21453–21458.
- 5 R. Borrego-Varillas, A. Nenov, P. Kabaciński, I. Conti, L. Ganzer, A. Oriana, V. K. Jaiswal, I. Delfino, O. Weingart, C. Manzoni, I. Rivalta, M. Garavelli and G. Cerullo, Tracking excited state decay mechanisms of pyrimidine nucleosides in real time, *Nat Commun*, 2021, **12**, 7285.
- 6 Y. Zhang, K. De La Harpe, A. A. Beckstead, L. Martínez-Fernández, R. Improtá and B. Kohler, Excited-State Dynamics of DNA Duplexes with Different H-Bonding Motifs, *J. Phys. Chem. Lett.*, 2016, **7**, 950–954.
- 7 S. Boldissar and M. S. De Vries, How nature covers its bases, *Phys. Chem. Chem. Phys.*, 2018, **20**, 9701–9716.
- 8 B. Marchetti, T. N. V. Karsili, M. N. R. Ashfold and W. Domcke, A ‘bottom up’, ab initio computational approach to understanding fundamental photophysical processes in nitrogen containing heterocycles, DNA bases and base pairs, *Phys. Chem. Chem. Phys* 2016, **18**, 20007–20027.
- 9 D. Nachtigallová, A. J. A. Aquino, J. J. Szymczak, M. Barbatti, P. Hobza and H. Lischka, Nonadiabatic Dynamics of Uracil: Population Split among Different Decay Mechanisms, *J. Phys. Chem. A*, 2011, **115**, 5247–5255.
- 10 S. Perun, A. L. Sobolewski and W. Domcke, Conical Intersections in Thymine, *J. Phys. Chem. A*, 2006, **110**, 13238–13244.
- 11 S. Matsika, Radiationless Decay of Excited States of Uracil through Conical Intersections, *J. Phys. Chem. A*, 2004, **108**, 7584–7590.
- 12 A. Yoshikawa and S. Matsika, Excited electronic states and photophysics of uracil–water complexes, *Chemical Physics*, 2008, **347**, 393–404.
- 13 R. Improtá, F. Santoro and L. Blancafort, Quantum Mechanical Studies on the Photophysics and the Photochemistry of Nucleic Acids and Nucleobases, *Chem. Rev.*, 2016, **116**, 3540–3593.
- 14 S. Saha and H. M. Quiney, Solvent effects on the excited state characteristics of adenine–thymine base pairs, *RSC Adv.*, 2017, **7**, 33426–33440.
- 15 H. Kang, K.T. Lee, S.K. Kim, Femtosecond real time dynamics of hydrogen bond dissociation in photoexcited adenine–water clusters, *Chemical physics letters*, 2002, **359**, 213–219.
- 16 B. Barc, M. Ryszka, J-C. Pouilly, E. Jabbour Al Maalouf, Z. El Otell, J. Tabet, R. Parajuli et al., Multi-photon and electron impact ionisation studies of reactivity in adenine–water clusters, *International Journal of Mass Spectrometry*, 2014, **365**, 194–199.
- 17 K. Sakota, A. Hara and H. Sekiya, Excited-state double-proton transfer dynamics of deuterated 7-azaindole dimers in a free jet studied by hole-burning spectroscopy, *Phys. Chem. Chem. Phys.*, 2004, **6**, 32.
- 18 H. Sekiya and K. Sakota, Excited-state double-proton transfer in a model DNA base pair: Resolution for stepwise and concerted mechanism controversy in the 7-azaindole dimer revealed by frequency- and time-resolved spectroscopy, *Journal of Photochemistry and Photobiology C: Photochemistry Reviews*, 2008, **9**, 81–91.
- 19 K. Sakota, C. Okabe, N. Nishi and H. Sekiya, Excited-State Double-Proton Transfer in the 7-Azaindole Dimer in the Gas Phase. 3. Reaction Mechanism Studied by Picosecond Time-Resolved REMPI Spectroscopy, *J. Phys. Chem. A*, 2005, **109**, 5245–5247.
- 20 K. Tokumura, Y. Watanabe, M. Udagawa and M. Itoh, Photochemistry of transient tautomer of 7-azaindole hydrogen-bonded dimer studied by two-step laser excitation fluorescence measurements, *J. Am. Chem. Soc.*, 1987, **109**, 1346–1350.
- 21 J. Catalán and M. Kasha, Photophysics of 7-Azaindole, Its Doubly-H-Bonded Base-Pair, and Corresponding Proton-Transfer-Tautomer Dimeric Species, via Defining Experimental and Theoretical Results, *J. Phys. Chem. A*, 2000, **104**, 10812–10820.
- 22 J. Catalán, J. C. Del Valle and M. Kasha, Resolution of concerted versus sequential mechanisms in photo-induced double-proton transfer reaction in 7-azaindole H-bonded dimer, *Proc. Natl. Acad. Sci. U.S.A.*, 1999, **96**, 8338–8343.
- 23 R. Crespo-Otero, N. Kungwan and M. Barbatti, Stepwise double excited-state proton transfer is not possible in 7-azaindole dimer, *Chem. Sci.*, 2015, **6**, 5762–5767.
- 24 K. Sakota, N. Komure, W. Ishikawa and H. Sekiya, Spectroscopic study on the structural isomers of 7-azaindole(ethanol)_n (n=1–3) and multiple-proton transfer reactions in the gas phase, *The Journal of Chemical Physics*, 2009, **130**, 224307.
- 25 K. Sakota, C. Jouvet, C. Dedonder, M. Fujii and H. Sekiya, Excited-State Triple-Proton Transfer in 7-Azaindole(H₂O)₂ and Reaction Path Studied by Electronic Spectroscopy in the Gas Phase and Quantum Chemical Calculations, *J. Phys. Chem. A*, 2010, **114**, 11161–11166.
- 26 K. Sakota, N. Inoue, Y. Komoto and H. Sekiya, Cooperative Triple-Proton/Hydrogen Atom Relay in 7-Azaindole(CH₃OH)₂ in the Gas Phase: Remarkable Change in the Reaction Mechanism from Vibrational-Mode Specific to Statistical Fashion with Increasing Internal Energy, *J. Phys. Chem. A*, 2007, **111**, 4596–4603.
- 27 J.-Y. Shen, W.-C. Chao, C. Liu, H.-A. Pan, H.-C. Yang, C.-L. Chen, Y.-K. Lan, L.-J. Lin, J.-S. Wang, J.-F. Lu, S. Chun-Wei Chou, K.-C. Tang and P.-T. Chou, Probing water micro-solvation in proteins by water catalysed proton-transfer tautomerism, *Nat Commun*, 2013, **4**, 2611.
- 28 S. Baweja, B. Kalal and S. Maity, Laser spectroscopic characterization of supersonic jet cooled 2,7-diazaindole, *Phys. Chem. Chem. Phys.*, 2023, **25**, 26679–26691.
- 29 S. Baweja, P. R. Chowdhury and S. Maity, Excited state hydrogen atom transfer pathways in 2,7-diazaindole – S1-3 (S = H₂O and NH₃) clusters, *Spectrochimica Acta Part A: Molecular and Biomolecular Spectroscopy*, 2022, **265**, 120386.
- 30 K. Fuke, H. Yoshiuchi and K. Kaya, Electronic spectra and tautomerism of hydrogen-bonded complexes of 7-azaindole in a supersonic jet, *J. Phys. Chem.*, 1984, **88**, 5840–5844.
- 31 S. Maity, R. Knochenmuss, C. Holzer, G. Féraud, J. Frey, W. Klopffer and S. Leutwyler, Accurate dissociation energies of two isomers of the 1-naphtho-cyclopropane complex, *J. Chem. Phys.*, 2016, **145**, 164304.
- 32 S. G. Balasubramani, G. P. Chen, S. Coriani, M. Diedenhofen, M. S. Frank, Y. J. Franzke, F. Furche, R. Grotjahn, M. E. Harding, C. Haüttig, A. Hellweg, B. Helmich-Paris, C. Holzer, U. Huniar, M. Kaupp, A. Marefat Khah, S. Karbalaei Khani, T. Müller, F. Mack, B. D. Nguyen, S. M. Parker, E. Perlt, D. Rappoport, K. Reiter, S. Roy, M. Ručkert, G. Schmitz, M. Sierka, E. Tapavicza, D. P. Tew, C. van Wuillen, V. K. Voora, F. Weigend, A. Wodyński and J. M. Yu, TURBOMOLE: Modular program suite for ab initio quantum-chemical and condensed-matter simulations, *J. Chem. Phys.*, 2020, **152**, 184107.
- 33 I. Pugliesi and K. Müller-Dethlefs, The use of multidimensional Franck–Condon simulations to assess model chemistries: A case study on phenol, *J. Phys. Chem. A*, 2006, **110**, 4657–4667.
- 34 S. Khodia and S. Maity, A combined experimental and computational study on the deactivation of a photo-excited 2,2'-pyridylbenzimidazole–water complex via excited-state proton transfer, *Phys. Chem. Chem. Phys.*, 2022, **24**, 12043–12051.

- 35 R. Jarupula, S. Khodia, M. Shabeeb and S. Maity, A combined spectroscopic and computational investigation on the solvent-to-chromophore excited-state proton transfer in the 2,2'-pyridylbenzimidazole–methanol complex, *Phys. Chem. Chem. Phys.*, 2023, **25**, 17010–17020.
- 36 H. Yokoyama, H. Watanabe, T. Omi, S. Ishiuchi, and M. Fujii, Structure of Hydrogen-Bonded Clusters of 7-Azaindole Studied by IR Dip Spectroscopy and ab Initio Molecular Orbital Calculation, *J. Phys. Chem. A*, 2001, **105**, 9366–9374.
- 37 K. Sakota and H. Sekiya, Probe of the NH Bond Strength in $1A$ and $1B$ States of 7-azaindole with IR-Dip Spectroscopy: Insights into the Electronic-State Dependence of the Multiple Proton/Hydrogen Transfers in Hydrogen-Bonded Clusters, *J. Phys. Chem. A*, 2009, **113**, 2663–2665.
- 38 *NIST Chemistry WebBook, NIST Standard Reference Database Number 69*, ed. P. J. Linstrom and W. G. Mallard, National Institute of Standards and Technology, Gaithersburg MD, 20899, 2021.
- 39 A. Nakajima, K. Ishikawa, M. Baba and K. Kaya, Spectroscopic study of Hydrogen bonded 7-Azaindole Clusters, *Laser Chem.*, 1995, **15**, 167–181.
- 40 O. Plekan, H. Sa'adeh, A. Ciavardini, C. Callegari, G. Cautero, C. Dri and M. D. Fraia, et al., Experimental and theoretical photoemission study of indole and its derivatives in the gas phase, *J. Phys. Chem. A*, 2020, **124**, 4115–4127.
- 41 K. Fuke, H. Yoshiuchi, K. Kaya, Y. Achiba, K. Sato, K. Kimura, Multiphoton ionization photoelectron spectroscopy and two-color multiphoton ionization threshold spectroscopy on the hydrogen bonded phenol and 7-azaindole in a supersonic jet, *Chemical physics letters*, 1984, **108**, 179–184.